

Unified framework for detecting phase synchronization in coupled time seriesJunfeng Sun^{1,2,*} and Michael Small²¹*Med-X Research Institute, Shanghai Jiao Tong University, 1954 Hua Shan Road, Shanghai 200030, China*²*Department of Electronic and Information Engineering, Hong Kong Polytechnic University, Kowloon, Hong Kong, China*

(Received 5 June 2009; published 27 October 2009)

Phase synchronization (PS) has drawn increasing attention in recent years for its extensive applications in analyzing time series observed from coupled systems. In this paper, we examine the detection of PS in bivariate time series from the viewpoints of signal processing and circular statistics. Several definitions of instantaneous phase (IP) are first revisited and further unified into a framework, which defines IP as the argument of the signal with a specific bandpass filter applied. With this framework, the constraints for IP definition are discussed and the effect of noise in IP estimation is studied. The estimate error of IP, which is due to noise, is shown to obey a scale mixture of normal (SMN) distributions. Further, under the assumption that the SMN of IP error can be approximated by a particular normal distribution, the estimate of mean phase coherence of bivariate time series is shown to be degraded by a factor, which is determined by only the level of in-band noise. Finally, simulations are provided to support the theoretical results.

DOI: [10.1103/PhysRevE.80.046219](https://doi.org/10.1103/PhysRevE.80.046219)

PACS number(s): 05.45.Xt, 05.45.Pq, 05.45.Tp

I. INTRODUCTION

Synchronization is a cooperative behavior, which means that the coupled systems evolve with the same rhythm. It is ubiquitous in both natural and engineering systems. Examples include coupled chaotic oscillators [1], human brain activities and muscle activities [2], neuronal oscillations [3,4], chaotic laser arrays [5], electrochemical oscillations [6], and coupled nanomechanical oscillators [7]. This phenomenon can not only reveal the mechanism and function of the coupled systems (e.g., communication during cognitive processing in human brain [3]) but also helps to gain new applications such as clinical treatment for Parkinson disease [8]. Therefore, it has drawn increasing attention in recent years (for a review, cf. Refs. [9,10]).

There are several different types of synchronization, such as complete synchronization (CS), generalized synchronization (GS), and phase synchronization (PS) [11]. Note that it is difficult to apply CS and GS to analyze bivariate time series observed from experimental systems. Nevertheless, PS, a weaker form of synchronization, is a suitable tool for observed time series and has been extensively applied. Let $\phi_{1,2}(t)$ denote the instantaneous phases (IP) of two coupled systems, respectively. Then the coupled systems are said to be in PS when the inequality $|l\phi_1(t) - m\phi_2(t)| < \text{const}$ holds, where l and m are positive integers. When $l:m=1:1$, the $l:m$ PS reduces to be the most straightforward form, i.e., 1:1 PS. Various methods have been introduced to detect synchronization [12–14]. However, to reliably detect synchronization is not so easy, especially for the case when one has only the observed time series, which are noncoherent (i.e., with broad power spectra) and unavoidably contaminated by noise [12,15,16]. The performance of various synchronization indexes, including PS indexes, can be greatly degraded when the noise level is relatively high [15]. Usually, the noisy data are prefiltered with a bandpass filter. A data-driven optimal

filter has been designed for noisy data in IP estimation [17] and some other algorithms have also been proposed to provide robust detection of PS in noisy data [14,18].

To detect PS in observed time series, an appropriate definition of IP is very important. Various definitions of IP have been introduced. Most of them are based on particular transforms, such as the Hilbert transform [1], the derivative of the Hilbert transform [6], a generalized transform with Gaussian filter [5], and the wavelet transform [19], of the observed data. To the best of our knowledge, although various definitions have been proposed, there are still several key points left to be addressed. The first problem is how to treat noncoherent data [20]. For noncoherent data, negative instantaneous frequency (IF) (defined as the derivative of IP with respect to time), which is physically meaningless, may be introduced by the Hilbert transform [21,22]. Usually, a narrow bandpass filter is applied as preprocessing. Then the first problem becomes what type of filter should be used. The second problem concerns the relationship among the various definitions of IP. To date, these IP definitions have been compared numerically with both simulation data and experimental signals [12,15]. However, their relationship has not been well understood theoretically. Beyond the suggestions given by numerical comparison, the puzzle of which IP definition is more appropriate for analyzing particular signals still exists. The third problem is how, quantitatively, the noise will affect the detection of PS. For contaminated data, artificial phase slips, introduced by noise, will reduce the reliability of the estimated PS index. A bandpass prefiltering may suppress the effect of noise but may introduce spurious overestimation of PS index as well [23]. Thus, an analytical study on the effect of noise is greatly desired.

In this paper, the above problems are treated from the viewpoints of signal processing and circular statistics. Several definitions of IP are revisited and further unified into a framework, which defines IP as the argument of the signal with a specific bandpass filter applied. With this framework, the constraints for IP definition are examined based on the theory of signal processing, and the relationship among several IP definitions is demonstrated. Furthermore, an analyti-

*jfsun@sjtu.edu.cn

cal study of the effect of noise in IP estimation and PS detection is given. The distribution of the IP error induced by noise is shown to be a scale mixture of normal (SMN) distributions. Under the assumption that the SMN of IP error can be approximated by a particular normal distribution, the estimate of PS index is shown to be degraded by a factor, which is determined by only the noise level in the pass band. Finally, these theoretical results are verified by numerical simulations.

The organization of this paper is as follows. In Sec. II, several definitions of IP are revisited and relevant comments are given. In Sec. III, a framework of IP definition is introduced, the constraints for IP definition are examined, and the relationship between IP and the Fourier transform is discussed. In Sec. IV, an analytical study of the effect of noise in IP estimation and PS detection is given. In Sec. V, simulations are performed to verify the analytical study on the effect of noise. Finally, a conclusion is given in Sec. VI.

II. REVISITING THE DEFINITION OF IP

In this section, we will revisit four definitions of IP and show that the IPs are actually defined as the arguments of the outputs of specific filters which are applied to the original observed signal. The differences of these IP definitions are the forms of the corresponding filters.

A. Definition of IP based on the Hilbert transform

The most popular definition of IP is based on the Hilbert transform. Given an observable signal $s(t)$, its analytic signal is defined as

$$s^{(h)}(t) = s(t) + j\tilde{s}(t) = A^{(h)}(t)e^{j\phi^{(h)}(t)}, \tag{1}$$

where

$$\tilde{s}(t) = \mathcal{H}[s(t)] = \frac{1}{\pi} \text{PV} \int_{-\infty}^{\infty} \frac{s(\tau)}{t - \tau} d\tau \tag{2}$$

is the Hilbert transform of $s(t)$ (here PV means that the integral is taken in the sense of Cauchy principal value), $A^{(h)}(t)$ is the instantaneous amplitude (IA), and $\phi^{(h)}(t)$, which is given by

$$\phi^{(h)}(t) = \arg[s^{(h)}(t)] = \arctan \frac{\tilde{s}(t)}{s(t)}, \tag{3}$$

is the IP of signal $s(t)$. The analytic signal $s^{(h)}(t)$ can be written as the convolution of $s(t)$ with a complex-response filter, i.e., $s^{(h)}(t) = s(t) * b^{(h)}(t)$, where $b^{(h)}(t) = \delta(t) + j\frac{1}{\pi t}$. In the frequency domain, $s^{(h)}(t)$ is $S^{(h)}(f) = S(f)B^{(h)}(f)$, where $S(f)$ and $B^{(h)}(f)$ are the Fourier transform of $s(t)$ and $b^{(h)}(t)$, respectively. By definition, the analytic signal can be obtained in the frequency domain by setting the negative frequency components of the Fourier transform of signal $s(t)$ to be zero and doubling the amplitudes of the positive frequency components, that is, the filter $B^{(h)}(f)$ should be

$$B^{(h)}(f) = \begin{cases} 2 & \text{if } f > 0 \\ 1 & \text{if } f = 0 \\ 0 & \text{if } f < 0. \end{cases} \tag{4}$$

For coherent data (i.e., with one dominating frequency component), the so-defined IP increases monotonically, while for noncoherent data, the so-defined IP may decrease at some instants and, thus, the corresponding IF may be negative, which is physically meaningless [21,22]. For this case, IP is not a one-to-one transformation to the analytic trajectory and ambiguity occurs in PS detection [18,20].

B. Definition of IP based on the idea of curvature

To deal with noncoherent data, some other IP definitions have been proposed. One of them defines IP as the argument of the derivative of the analytic signal $s^{(h)}(t)$, i.e., $\phi^{(d)}(t) = \arg[s^{(d)}(t)]$, where $s^{(d)}(t) = \frac{ds(t)}{dt} + j\frac{d\tilde{s}(t)}{dt}$ [6]. We can write $s^{(d)}(t)$ as $s^{(d)}(t) = \frac{ds^{(h)}(t)}{dt} = \frac{d}{dt}[s(t) * (\delta(t) + j\frac{1}{\pi t})] = s(t) * \frac{d}{dt}[\delta(t) + j\frac{1}{\pi t}] = s(t) * b^{(d)}(t)$, where $b^{(d)}(t) = \delta'(t) - j\frac{1}{\pi t^2}$. In the frequency domain, $s^{(d)}(t)$ appears as $S^{(d)}(f) = S(f)B^{(d)}(f)$, where

$$B^{(d)}(f) = \begin{cases} j4\pi f & \text{if } f > 0 \\ j2\pi f & \text{if } f = 0 \\ 0 & \text{if } f < 0 \end{cases} \tag{5}$$

is the Fourier transform of $b^{(d)}(t)$. Obviously, this filter amplifies the high-frequency components. Note that this IP definition is based on the idea of the curvature of an arbitrary curve [24]. If the curvature of curve $C_1 = [s(t), \tilde{s}(t)]$, which is defined in the $[s(t), \tilde{s}(t)]$ plane, is positive, the curve $C_2 = [\frac{ds(t)}{dt}, \frac{d\tilde{s}(t)}{dt}]$ will cycle monotonically around a fixed point and, thus, the IP $\phi^{(d)}(t) = \arg[s^{(d)}(t)]$ will increase monotonically. However, for noncoherent data, the curvature of curve C_1 is not always positive. For the instants the curvature turns from positive to negative, the corresponding IP will decrease. Thus, this definition is not always applicable to arbitrary noncoherent data.

C. Definition of IP with Gaussian filter

As discussed above, the analytic signal is obtained by applying a specific filter to the real signal $s(t)$. With this fact, a generalized definition of IP is proposed by applying a Gaussian filter (its envelope is a Gaussian function and thus named) $b^{(g)}(t) = \frac{1}{\sqrt{2\pi}T} e^{-t^2/(2T^2)} e^{j2\pi f_n t}$ to $s(t)$, i.e., $s^{(g)}(t) = s(t) * b^{(g)}(t)$ [5]. In the frequency domain, $s^{(g)}(t)$ turns out to be $S^{(g)}(f) = S(f)B^{(g)}(f)$, where

$$B^{(g)}(f) = e^{-2\pi^2 T^2 (f - f_n)^2}. \tag{6}$$

Actually, $b^{(g)}(t)$ is a narrow-band Gaussian filter [i.e., $\frac{1}{\sqrt{2\pi}T} e^{-t^2/(2T^2)}$], which is shifted by the nominal frequency f_n in

the frequency domain.¹ Then the IP is defined as $\phi^{(g)}(t) = \arg[s^{(g)}(t)]$. This definition has been applied successfully in detecting PS of coupled laser arrays, which the method based on the Hilbert transform has failed to reveal [5]. This is because PS only exists between the components in a particular frequency band of the laser data. If these components are not extracted by a bandpass filter, PS between them will be submerged by noise and the components in other bands and thus cannot be detected.

D. Definition of IP based on the wavelet transform

One more IP definition is based on the wavelet transform [19]. With the Gabor wavelet $\psi(t) = g(t)e^{j2\pi vt}$, the wavelet transform of $s(t)$ is $s^{(w)}(u, a) = \int_{-\infty}^{\infty} s(t) \frac{1}{\sqrt{a}} \psi^*\left(\frac{t-u}{a}\right) dt$, where $g(t) = (T^2\pi)^{-1/4} e^{-t^2/(2T^2)}$ is the envelope. Let $b_a^{(w)}(t) = \frac{1}{\sqrt{a}} \psi^*\left(\frac{t}{a}\right)$, then

$$s^{(w)}(u, a) = \int_{-\infty}^{\infty} s(t) b_a^{(w)}(u-t) dt = s(u) * b_a^{(w)}(u),$$

where

$$b_a^{(w)}(u) = \frac{1}{\sqrt{a}} g\left(\frac{-u}{a}\right) e^{j2\pi vu/a} = \frac{1}{\sqrt{a}} g\left(\frac{u}{a}\right) e^{j2\pi vu/a}$$

because $g(t)$ is symmetrical. Let $f_n = \frac{\nu}{T}$ and $\nu=1$. Then $s^{(w)}(u, a) = s(u) * b^{(w)}(u)$, where $b^{(w)}(u) = f_n^{1/2} g(f_n u) e^{j2\pi f_n u}$. The difference between $b^{(w)}(t) = f_n^{1/2} (T^2\pi)^{-1/4} e^{-t^2 f_n^2 / (2T^2)} e^{j2\pi f_n t}$ and $b^{(g)}(t) = \frac{1}{\sqrt{2\pi T}} e^{-t^2 / (2T^2)} e^{j2\pi f_n t}$ is the amplitude and the width of the Gaussian window, that is, $b^{(w)}(t)$ is scaled by f_n . In the frequency domain, $g(t)$ appears as $G(f) = (4\pi T^2)^{1/4} e^{-2\pi^2 f^2 T^2}$, and $b^{(w)}(t)$ is

$$B^{(w)}(f) = f_n^{-1/2} G\left(\frac{f}{f_n} - 1\right). \quad (7)$$

Therefore, this method obtains the analytic signal by applying a scaled bandpass filter to the signal $s(t)$.

III. FRAMEWORK FOR IP DEFINITION

In this section, we first show that the IP definitions discussed above can be unified into one common framework: applying a particular filter to the observable signal $s(t)$ and further defining the IP as the argument of the output of the filter. Furthermore, we study the constraints for defining IP and the requirements for the filter. After that, we discuss the relation between the so-defined IP and the Fourier transform from the viewpoint of signal processing.

A. Defining IP with bandpass filter

In the field of signal processing, IF, which is commonly defined as the derivative of IP, is an important concept and

¹The nominal frequency denotes the midpoint in the pass band or the arithmetic mean between the high and the low cut-off frequencies of the filter. It also denotes the desired center frequency of a crystal or oscillator.

has been widely studied [25–27]. The filter $b(t) = g(t)e^{j2\pi f_n t}$, which has a complex response, has been introduced to estimate IP [28], where $g(t) = \frac{1}{\sqrt{2\pi T}} e^{-t^2 / (2T^2)}$ is the envelope of the filter and T is the response duration. In the frequency domain, $b(t)$ is

$$B(f) = \int_{-\infty}^{\infty} b(t) e^{-j2\pi f t} dt = \int_{-\infty}^{\infty} g(t) e^{-j2\pi(f-f_n)t} dt = G(f-f_n), \quad (8)$$

where $G(f) = e^{-2\pi^2 f^2 T^2}$ is the Fourier transform of $g(t)$. When the signal $s(t)$ is passed through this filter, the output of the filter, i.e., $s^{(b)}(t) = s(t) * b(t)$, is analytic if the bandwidth of the filter is smaller than $2f_n$ [28], since its spectra at negative frequencies are eliminated by the bandpass filter.² Then IP is defined as $\phi^{(b)}(t) = \arg[s^{(b)}(t)]$. If the envelope $g(t)$ is a Gaussian function, this method is exactly the one based on a Gaussian filter, which has been introduced in Sec. II C. Of course, some other windows, such as the Hamming window, can be used as the envelope as well. No matter what filter is used, it is applied to constrain the output of the filter to be coherent, i.e., narrow band with only one prominent spectral component.

The analytic signal $s^{(b)}(t) = s(t) * b(t)$ can be interpreted as a combination of the Hilbert transform and a real bandpass filter. Let $s^{(r)}(t) = s(t) * \mathcal{R}[b(t)] = s(t) * [g(t)\cos(2\pi f_n t)]$, where $\mathcal{R}(\cdot)$ denotes the real part of the complex variable (\cdot) . In the frequency domain, $s^{(r)}(t)$ appears as

$$S^{(r)}(f) = S(f) \left[\frac{1}{2} G(f+f_n) + \frac{1}{2} G(f-f_n) \right]. \quad (9)$$

As Eq. (4) indicates, the analytic signal of $s^{(r)}(t)$ can be obtained in the frequency domain by eliminating the negative frequency components of $s^{(r)}(t)$ but doubling the amplitudes of the positive frequency components. Therefore, the analytic signal of $s^{(r)}(t)$ can be obtained by the inverse Fourier transform of $S^{(r)}(f)B^{(h)}(f)$, i.e.,

$$\begin{aligned} & \mathcal{F}^{-1}[S^{(r)}(f)B^{(h)}(f)] \\ &= \mathcal{F}^{-1}\left\{ S(f) \left[\frac{1}{2} G(f+f_n) + \frac{1}{2} G(f-f_n) \right] B^{(h)}(f) \right\} \\ &= \mathcal{F}^{-1}[S(f)G(f-f_n)] = s(t) * \mathcal{F}^{-1}[G(f-f_n)] \\ &= s(t) * [g(t)e^{j2\pi f_n t}] = s^{(b)}(t), \end{aligned} \quad (10)$$

where $\mathcal{F}^{-1}(\cdot)$ denotes the inverse Fourier transform operator.

B. Constraints for IP definition

In the sections above, it is shown that IP can be defined as the argument of the signal with a particular filter applied.

²Note that here we consider that the frequency components outside the pass band are completely eliminated. For real implementation of filter, the frequency components outside the pass band may not be eliminated completely but suppressed to a very low level. So, precisely speaking, $s^{(b)}(t)$ only approximates an analytic signal. The approximation error has been discussed in Refs. [29,30].

Then are there any constraints for the filter in defining IP? In this section, we will address this problem from the viewpoint of signal processing.

The signal $s(t)$ can be written as $s(t) = \mathcal{R}[A(t)e^{j\phi(t)}]$, i.e., the real part of a complex variable. Usually, the corresponding imaginary counterpart $\mathcal{I}[A(t)e^{j\phi(t)}]$ cannot be observed and is assumed to relate to $s(t)$ by a certain operation, i.e., $\mathcal{I}[A(t)e^{j\phi(t)}] = \tilde{\mathcal{H}}[s(t)]$. To define IP, various operators $\tilde{\mathcal{H}}(\cdot)$ have been proposed and the Hilbert transform $\mathcal{H}(\cdot)$ is the most popular one. Three physical conditions have been proposed to constrain the operator $\tilde{\mathcal{H}}(\cdot)$ [25]:

(i) Condition I: amplitude continuity and differentiability. This condition guarantees that the associated amplitude $A(t)$ is continuous and differentiable.

(ii) Condition II: phase independence of scaling and homogeneity. This condition means that the IPs of signals $s(t)$ and $c \cdot s(t)$ are the same. In other words, this condition requires that the operator possesses the property $\tilde{\mathcal{H}}[cs(t)] = c\tilde{\mathcal{H}}[s(t)]$.

(iii) Condition III: harmonic correspondence. This condition requires that for any constant amplitude $A > 0$, frequency $\omega > 0$, and phase ψ , the operator satisfies $\tilde{\mathcal{H}}[A \cos(\omega t + \psi)] = A \sin(\omega t + \psi)$.

The Hilbert transform $\mathcal{H}(\cdot)$ has been proven to be the only one that satisfies these physical conditions [25]. Considering this, we only investigate the IP definition based on the Hilbert transform in this paper. More discussions in these conditions can be found in Ref. [25].

For a coherent signal, the Hilbert transform works well and the so-defined IP [Eq. (3)] increases monotonically. But for a noncoherent signal, the corresponding IP no longer increases monotonically, resulting in negative IF at some instants, which is physically meaningless. This problem can be addressed with the Bedrosian theorem [29,30]. This theorem states that for a low-frequency term $l(t)$ and a high-frequency term $h(t)$, which have no spectra overlapping, the relation

$$\mathcal{H}[l(t)h(t)] = l(t)\mathcal{H}[h(t)] \quad (11)$$

holds; that is, the low-frequency term can be taken out of the Hilbert transform. For a signal of the form $s(t) = A(t)\cos \phi(t)$, $A(t)$ and $\cos \phi(t)$ correspond to the low-frequency term $l(t)$ and the high-frequency term $h(t)$, respectively. Straightforwardly, a complex form of signal $s(t)$ is defined as $s_q(t) = A(t)e^{j\phi(t)}$, which is called the *quadrature model* of $s(t)$. This model is used before the introduction of the concept of analytic signal. It seems natural to take $\phi(t)$ as IP. However, this model does not tell how to estimate $A(t)$ and $\phi(t)$ from only the observable signal $s(t)$ and thus is difficult to be applied to observed time series. There is a difference between $s_q(t)$ and the analytic signal $s^{(h)}(t)$ [Eq. (1)], which is estimated with the Hilbert transform. The energy of the difference is twice the energy of the negative frequency components of the quadrature model [30]. This difference tends to vanish as $A(t)$ and $\cos \phi(t)$ fulfill the Bedrosian theorem. In other words, the more noncoherent the signal (i.e., the broader of the spectra of the signal), the bigger the difference. Condition II, i.e., $\tilde{\mathcal{H}}[cs(t)] = c\tilde{\mathcal{H}}[s(t)]$, sets a constraint on the operator. Additionally, the Bedrosian

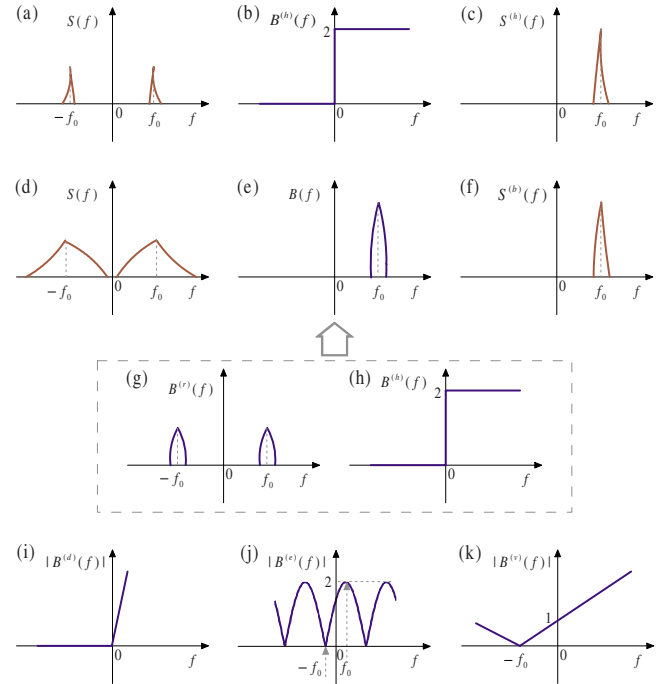


FIG. 1. (Color online) Schematic diagram of IP definitions. (a) $S(f)$, the Fourier transform of a coherent signal $s(t)$; (b) $B^{(h)}(f)$, the filter for IP definition based on the Hilbert transform [Eq. (4)]; (c) $S^{(h)}(f) = S(f)B^{(h)}(f)$, the Fourier transform of the analytic signal $s^{(h)}(t) = s(t) * b^{(h)}(t)$; (d) $S(f)$, the Fourier transform of a noncoherent signal; (e) $B(f)$, a narrow bandpass complex-response filter with nominal frequency f_0 [Eq. (8)]; (f) $S^{(b)}(f) = S(f)B(f)$, the Fourier transform of the analytic signal $s^{(b)}(t) = s(t) * b(t)$; (g) $B^{(r)}(f)$, the Fourier transform of $g(t)\cos(2\pi f_0 t)$, i.e., the filter $b(t) = \mathcal{R}[g(t)e^{j2\pi f_0 t}]$; (h) $B^{(h)}(f)$; (i) $|B^{(d)}(f)|$ [Eq. (5)], the complex-response filter for IP definition based on the idea of curvature; (j) $|B^{(e)}(f)|$, where $B^{(e)}(f) = 1 - je^{j2\pi f\tau}$, $f_0 = \frac{1}{4\tau}$; and (k) $|B^{(v)}(f)|$, where $B^{(v)}(f) = 1 + 2\mu\pi f$, $f_0 = \frac{1}{2\mu\pi}$.

theorem sets a constraint, which is similar to condition II, to the signal. If the low-frequency term $l(t)$ is a constant, then $\mathcal{H}[cs(t)] = c\mathcal{H}[s(t)]$ obviously holds.

To fulfill the Bedrosian theorem, we apply a bandpass filter $b(t)$ to the noncoherent signal, i.e., $s^{(b)}(t) = s(t) * b(t)$, so that the filtered signal is coherent. For the filtered signal, its IA $A^{(b)}(t)$ varies much more slowly than $\cos \phi^{(b)}(t)$, which means that the effective frequency band of $A^{(b)}(t)$ is much lower than that of $\cos \phi^{(b)}(t)$ [30]. The effective bandwidth of the filter $b(t)$ is $\Delta f = 1/(2\sqrt{2}\pi T)$ [28]. To let the filtered signal fulfill the Bedrosian theorem, $\frac{\Delta f}{2}$ should be less than f_n , which gives $T > 1/(4\sqrt{2}\pi f_n)$. The IF $\frac{1}{2\pi} \frac{d\phi^{(b)}(t)}{dt}$ of the components in the pass band approaches the nominal frequency f_n in an asymptotic sense as the pass band of $b(t)$ becomes narrower to be a delta function, i.e., $\delta(f - f_n)$, in the frequency domain [26]. Note that for the method based on the wavelet transform, a similar theorem gives the constraint for estimating the analytic signal $s^{(w)}(t)$ ([31], p. 91–93).

Based on the three physical conditions and the Bedrosian theorem, we give some comments on several IP definitions with a schematic diagram (Fig. 1). For a coherent signal [Fig. 1(a)], the IP definition based on the Hilbert transform [Fig. 1(b)] is a proper choice for the signal itself fulfills the Bed-

rosian theorem, and the other three IP definitions introduced in Sec. II are also applicable, though they are not indeed required for a coherent signal. For a noncoherent signal [Fig. 1(d)], the Hilbert transform-based method no longer works well for the signal does not fulfill the Bedrosian theorem. In Sec. III A, a narrow complex-response bandpass filter [Fig. 1(e)] is applied to make the filtered signal coherent [Fig. 1(f)]. As we have demonstrated, this filter [i.e., $B(f)$, Eq. (8)] can be considered as the combination of $B^{(r)}(f)$ and $B^{(h)}(f)$, i.e., $B(f) = B^{(r)}(f)B^{(h)}(f)$ [Eqs. (9) and (10); Figs. 1(e), 1(g), and 1(h)]. Actually, the IP definition with Gaussian filter [Sec. II C; Eq. (6)] and the IP definition based on the wavelet transform [Sec. II D; Eq. (7)] are both similar with the IP definition with bandpass filter $B(f)$. The differences between these filters are the shape of the pass band of the filter. Thus, these two IP definitions work well for noncoherent signals if their bandwidths and nominal frequencies are properly set so that the filter can shape the original signals to be coherent.

The Hilbert transform has been proved to be the unique operator that satisfies the three physical conditions. For the IP definition based on the Hilbert transform, the filter $B^{(h)}(f)$ deletes all the negative frequency components of the Fourier transform of the real signal $s(t)$ to generate its analytic signal $s^{(h)}(t)$. So for any other IP definitions, the negative frequency components the complex signal generated from the real signal $s(t)$ must be zero, such as $S^{(h)}(f)$ in Fig. 1(c) and $S^{(b)}(f)$ in Fig. 1(f), before the argument of the complex signal can be defined as IP. Additionally, the Bedrosian theorem requires that the complex signal must be coherent, i.e., with narrow-band spectra. For a general noncoherent signal, we suggest that the IP can be defined by applying a complex-response bandpass filter as that proposed in Sec. III A.

For the IP definition based on the idea of curvature, the complex-response filter is $B^{(d)}(f)$ [Eq. (5)]. As Fig. 1(i) indicates, this filter deletes all the negative frequency components but amplifies the amplitudes of the positive high-frequency components. For a coherent signal, this IP definition works, though the amplification of the positive high-frequency components will lead the so-defined IP to be different from that defined by the method based on the Hilbert transform. For noncoherent signals, this definition may work for particular cases as have been reported [24], but it is not generally applicable for any case because the filter $B^{(d)}(f)$ does not assure that the filtered signal $s^{(d)}(t) = s(t) * b^{(d)}(t)$ is coherent.

Two variations in the generalized IP have been discussed in Ref. [5]. The first variation is with filter $B^{(e)}(f) = 1 - j e^{j2\pi f\tau}$. In the time domain, this filter is $b^{(e)}(t) = \delta(t) - j\delta(t + \tau)$, and $s^{(e)}(t) = s(t) * b^{(e)}(t) = s(t) - js(t + \tau)$. We can obtain $s^{(e)}(t) = s(t) + js(t + \tau)$ by changing the filter slightly to be $b^{(e)}(t) = \delta(t) + j\delta(t + \tau)$. Now the so-defined IP $\phi^{(e)}(t) = \arg[s^{(e)}(t)]$ can be interpreted as the angle of the reconstructed phase trajectory in the two-dimensional surface of time delay embedding, i.e., $[s(t), s(t + \tau)]$, where τ is the time delay [32]. As Fig. 1(j) indicates, the filter $B^{(e)}(f)$ can only eliminate the negative frequency components of the Fourier transform of signal $s(t)$ at the frequency bins $\frac{1}{\tau}(k - \frac{1}{4})$, where k is a nonpositive integer. So only for the coherent signal with spectra that locate at $\frac{1}{\tau}(k - \frac{1}{4})$, the filter

$B^{(e)}(f)$ can guarantee that the filtered signal fulfills the constraints for IP definition.

The second variation is with filter $B^{(v)}(f) = 1 + 2\mu\pi f$. In the time domain, this filter is $b^{(v)}(t) = \delta(t) - j\mu\delta'$. With $s^{(v)}(t) = s(t) * b^{(v)}(t) = s(t) - j\mu\frac{ds(t)}{dt}$, the IP is defined as $\phi^{(v)}(t) = \arg[s^{(v)}(t)]$. This definition is similar with the one defined by Mandelstam's method, which is widely used in the nonlinear oscillation theory [25]. Mandelstam's method defines IP in the plane $[s(t), -\frac{1}{2\pi f_n}\frac{ds(t)}{dt}]$, where f_n is the nominal frequency of the oscillation. When $\mu = \frac{1}{2\pi f_n}$, these two definitions are the same. Furthermore, if $\mu = 1$, $\phi^{(v)}(t)$ can be interpreted as the angle of the state of displacement versus velocity. However, as Fig. 1(k) indicates, the filter $B^{(v)}(f)$ does not suppress all the negative frequency components. Only for the signal of frequency $f = -\frac{1}{2\mu\pi}$, this IP definition satisfies the constraints for IP definition. For any other signal, this definition will introduce oscillation and distortion for the so-defined IP. More discussions on this IP definition can be found in Ref. [25] and references therein.

C. Relationship between IP and the Fourier transform

Under the assumption that $g(t)$ is symmetric, the analytic signal $s^{(b)}(t) = s(t) * b(t)$ can be written as

$$\begin{aligned} s^{(b)}(t) &= \int_{-\infty}^{\infty} s(u)b(t-u)du \\ &= \int_{-\infty}^{\infty} s(u)g(t-u)e^{j2\pi f_n(t-u)}du \\ &= e^{j2\pi f_n t} \int_{-\infty}^{\infty} s(u)g(u-t)e^{-j2\pi f_n u}du \\ &= e^{j2\pi f_n t} S_t(f) \Big|_{f=f_n}, \end{aligned} \quad (12)$$

where $S_t(f) = \int_{-\infty}^{\infty} s(u)g(u-t)e^{-j2\pi f u}du$ is the short-time Fourier transform of real signal $s(t)$ with symmetrical Gaussian window $g(t)$. Note that $S_t(f) \Big|_{f=f_n}$ is dependent on both time t and the nominal frequency f_n . If the bandwidth of $S_t(f)$ is much smaller than the nominal frequency f_n , the amplitude of $S_t(f) \Big|_{f=f_n}$ can be considered as the amplitude of the band-limited analytic signal $s^{(b)}(t)$. In other words, $s^{(b)}(t)$ can be considered as an amplitude-modulated signal with carrier frequency f_n and $S_t(f) \Big|_{f=f_n}$ corresponds to the low-frequency term that is required in Eq. (11). Then the IP can be written as

$$\phi^{(b)}(t) = \arg[s^{(b)}] = 2\pi f_n t + \arg[S_t(f) \Big|_{f=f_n}]. \quad (13)$$

Let us further examine two extreme cases of the bandpass filter $b(t)$. The first one is that the filter $b(t)$ is an all-pass filter, i.e., $g(t) = \delta(t)$. For this case, we have $b(t) = \delta(t)e^{j2\pi f_n t} = \delta(t)$ and $s^{(b)}(t) = s(t) * b(t) = s(t)$. As $s(t)$ is a real signal, $\arg[s^{(b)}(t)] = 0$, which gives no meaningful information of $s(t)$. The second extreme case is that the filter is $b(t) = g(t)e^{j2\pi f_n t}$ with envelope $g(t) = 1$. In the frequency domain, $g(t)$ turns out to be $G(f) = \delta(f)$, which means that the filter [i.e., $b(t) = e^{j2\pi f_n t}$] is extremely narrow and lets only the component of frequency f_n pass. Then we have

$$\begin{aligned}
 S_t(f)|_{f=f_n} &= \int_{-\infty}^{\infty} s(u)g(u-t)e^{-j2\pi f_n u} du \\
 &= \int_{-\infty}^{\infty} s(u)e^{-j2\pi f_n u} du \\
 &= \mathcal{F}[s(u)](f)|_{f=f_n}, \tag{14}
 \end{aligned}$$

where $\mathcal{F}[s(u)](f)$ denotes the Fourier transform of $s(u)$. From Eqs. (12) and (13), we get $s^{(b)}(t) = e^{j2\pi f_n t} \mathcal{F}[s(u)](f)|_{f=f_n}$ and $\phi^{(b)}(t) = 2\pi f_n t + \arg\{\mathcal{F}[s(u)](f)|_{f=f_n}\}$. For this case, $\arg\{\mathcal{F}[s(u)](f)|_{f=f_n}\}$ is dependent on f_n but not dependent on time t . The IF of the component in the pass band is $f_b(t) = \frac{1}{2\pi} \frac{d \arg[s^{(b)}]}{dt} = f_n$, which is actually the nominal frequency of the filter. This is obvious because

$$s^{(b)}(t) = s(t) * b(t) = \int_{-\infty}^{\infty} S(f) \delta(f - f_n) e^{j2\pi f t} df$$

is the component of frequency f_n , which is extracted from $s(t)$ by filter $b(t)$. As $g(t) \rightarrow 1$, the filter $b(t) \rightarrow e^{j2\pi f_n t}$, then the analytic signal $s^{(b)}(t)$ approaches to be $\int_{-\infty}^{\infty} S(f) \delta(f - f_n) e^{j2\pi f t} df$ in an asymptotic sense.

Note that the relationship of techniques based on the Hilbert transform, the wavelet transform, and the Fourier transform has also been discussed from other angles [12,33]. In Ref. [33], it is demonstrated that the spectral analysis based on the Hilbert transform, the wavelet transform, and the Fourier transform are “in fact formally (i.e., mathematically) equivalent when using the class of wavelets that is typically applied in spectral analysis.” This is true when the parameters of these three transforms are set in a particular way, and spectral analyses based on them turn out to be equivalent to each other. But for other cases, these three transforms have their own features and advantages for specific applications. It is not appropriate to claim that they are arbitrarily equivalent. Other discussions on the relationship between these transforms can be found in Refs. [26,33].

IV. EFFECT OF NOISE IN PS DETECTION

In real applications, the observable signal is contaminated more or less by noise. In this section, we perform an analytical study of the effect of noise in IP estimation and PS detection.

Let $s(t) = x(t) + w(t)$ denote the noisy signal, where $x(t)$ is the clean signal and $w(t)$ is the noise term. A bandpass filter $b(t)$ is first applied to the noisy signal $s(t)$, and the output can be written as

$$\begin{aligned}
 s^{(b)}(t) &= s(t) * b(t) \\
 &= x(t) * b(t) + w(t) * b(t) \\
 &= A_x(t) e^{j\phi_x^{(b)}(t)} + w^{(b)}(t), \tag{15}
 \end{aligned}$$

where $w^{(b)}(t) = w(t) * b(t)$. Let $\hat{\phi}_x^{(b)}(t)$ denote the estimate of $\phi_x^{(b)}(t)$ from the noisy signal $s(t)$ and $\theta(t) = \hat{\phi}_x^{(b)}(t) - \phi_x^{(b)}(t)$ denote the estimate error of IP due to the noise term $w(t)$. It

has been proved that the distribution of $\theta(t)$ is

$$\begin{aligned}
 p(\theta) &= \frac{\exp[-A_x^2/(2\sigma_w^{(b)})]}{2\pi} \\
 &+ \frac{A_x \cos \theta}{\sqrt{2\pi}\sigma_w^{(b)}} \operatorname{erf}\left[\frac{A_x \cos \theta}{\sigma_w^{(b)}}\right] \exp\left[\frac{-A_x^2 \sin^2 \theta}{2\sigma_w^{(b)}}\right], \tag{16}
 \end{aligned}$$

where the error function is defined by $\operatorname{erf}(x) = \frac{1}{\sqrt{2\pi}} \int_{-\infty}^x e^{-y^2/2} dy$ and $\sigma_w^{(b)}$ denotes the root mean square of $\mathcal{R}[w^{(b)}(t)]$ [34]. When the instantaneous signal-to-noise ratio (iSNR) $r^{(b)}(t) = A_x^2(t)/[2\sigma_w^{(b)}]$ in the pass band is large [$r^{(b)}(t) \geq 5$], the term $\exp[-A_x^2/(2\sigma_w^{(b)})]/(2\pi)$ in Eq. (16) is very small and can be neglected, the error function approximates unity, and $\sin \theta \approx \theta$, $\cos \theta \approx 1$, because $|\theta| \ll 1$. Then Eq. (16) is reduced to be a normal distribution, i.e., $\theta \sim N(0, \sigma_\theta^2)$,

$$p(\theta) = (\sqrt{2\pi}\sigma_\theta)^{-1} e^{-\theta^2/(2\sigma_\theta^2)}, \tag{17}$$

where $\sigma_\theta = \sigma_w^{(b)}/A_x(t)$. Since $\theta(t)$ is an angle, its distribution can be wrapped into $(-\pi, \pi)$ and turns out to be the wrapped normal (WN) distribution $\Theta \sim \tilde{N}(0, \sigma_\theta^2)$,

$$p(\Theta) = \frac{1}{\sqrt{2\pi}\sigma_\theta} \sum_{k=-\infty}^{\infty} e^{-(\Theta + 2k\pi)^2/(2\sigma_\theta^2)}, \tag{18}$$

where Θ stands for the wrapped θ , i.e., $\Theta = \theta \pmod{2\pi}$ [35,36].

The WN distribution possesses the reproductive property [36]. Specifically, if $\Theta_1 \sim \tilde{N}(\mu_1, \sigma_{\theta_1}^2)$ and $\Theta_2 \sim \tilde{N}(\mu_2, \sigma_{\theta_2}^2)$ are independent, the relation $(\Theta_1 - \Theta_2) \sim \tilde{N}(\mu_1 - \mu_2, \sigma_{\theta_1}^2 + \sigma_{\theta_2}^2)$ holds. Here, $\mu_1 = 0, \mu_2 = 0$, and thus $(\Theta_1 - \Theta_2) \sim \tilde{N}(0, \sigma_{\theta_1}^2 + \sigma_{\theta_2}^2)$. For the variables $x_{1,2}(t)$ of the coupled systems [e.g., Eq. (26)], their IPs, i.e., $\hat{\phi}_{x_{1,2}}^{(b)}(t)$, can be obtained. Let $\varphi = \phi_{x_1}^{(b)} - \phi_{x_2}^{(b)}$, $\hat{\varphi} = \hat{\phi}_{x_1}^{(b)} - \hat{\phi}_{x_2}^{(b)}$, $\theta_1 = \hat{\phi}_{x_1}^{(b)} - \phi_{x_1}^{(b)}$, and $\theta_2 = \hat{\phi}_{x_2}^{(b)} - \phi_{x_2}^{(b)}$ [for briefness, the variable t in formulas, such as $\phi_{x_1}^{(b)}(t)$, is omitted]. Then we have

$$\begin{aligned}
 \hat{\varphi} - \varphi &= [\hat{\phi}_{x_1}^{(b)} - \hat{\phi}_{x_2}^{(b)}] - [\phi_{x_1}^{(b)} - \phi_{x_2}^{(b)}] \\
 &= [\hat{\phi}_{x_1}^{(b)} - \phi_{x_1}^{(b)}] - [\hat{\phi}_{x_2}^{(b)} - \phi_{x_2}^{(b)}] \\
 &= \theta_1 - \theta_2. \tag{19}
 \end{aligned}$$

It is obvious that $(\hat{\varphi} - \varphi)$ turns out to be $(\Theta_1 - \Theta_2)$ when it is wrapped into $(-\pi, \pi)$ and thus obeys the WN distribution $\tilde{N}(0, \sigma_{\theta_1}^2 + \sigma_{\theta_2}^2)$.

Various PS indices have been proposed [12]. Two popular indices are based on entropy [2,23] and circular statistics [36,37], respectively. They both quantify how concentrated the distribution of IP difference is. In this paper, we adopt the

latter one,³ which is called mean phase coherence (MPC) and defined as $\rho = \|E[e^{j\varphi}]\|$. To deduce the effect of noise on the estimate of MPC, we first express the estimate of MPC for the noisy signal as

$$\hat{\rho} = \|E[e^{j\hat{\varphi}}]\| = \|E[e^{j(\hat{\varphi}-\varphi)}]\| = \|E[e^{j(\hat{\varphi}-\varphi)}]\| \cdot \|E[e^{j\varphi}]\|. \quad (20)$$

In statistics, the characteristic function (CHF) of a variable x is defined as $C_x(k) = \int_{-\infty}^{\infty} p(x) e^{jxk} dx$, where $p(x)$ is the probability density function (pdf) of variable x . Actually, CHF is the average value of e^{jxk} , i.e., $C_x(k) = E[e^{jxk}]$. If x obeys the WN distribution $x \sim \tilde{N}(\mu, \sigma^2)$, its CHF is $C_x(k) = e^{j\mu k - \sigma^2 k^2/2}$, where k is an integer [36,38]. As we have demonstrated that $(\hat{\varphi} - \varphi)$ obeys the WN distribution $\tilde{N}(0, \sigma_{\theta_1}^2 + \sigma_{\theta_2}^2)$ when it is wrapped into $(-\pi, \pi]$, we can get $C_{(\hat{\varphi}-\varphi)}(k) = e^{-(\sigma_{\theta_1}^2 + \sigma_{\theta_2}^2)k^2/2}$ [Eq. (19)]. Then from Eq. (20), we have

$$\hat{\rho} = \|C_{(\hat{\varphi}-\varphi)}(1)\| \cdot \|E[e^{j\varphi}]\| = e^{-(\sigma_{\theta_1}^2 + \sigma_{\theta_2}^2)/2} \rho, \quad (21)$$

which implies that the noise introduces a degrading factor, i.e., $e^{-(\sigma_{\theta_1}^2 + \sigma_{\theta_2}^2)/2}$, to the true index ρ , and this factor is determined by only the level of in-band noise.

Note that in Eqs. (16) and (17), A_x (as well as $\sigma_{\theta} = \sigma_{w^{(b)}}/A_x$) is a time-dependent variable, i.e., $A_x(t)$, if the amplitude of signal $s^{(b)}(t)$ is not a constant. So θ actually obeys a conditional distribution and Eq. (17) turns out to be

$$p(\theta|\sigma_{\theta}) = (\sqrt{2\pi}\sigma_{\theta})^{-1} e^{-\theta^2/(2\sigma_{\theta}^2)}, \quad \sigma_{\theta} > 0. \quad (22)$$

For the time series $\{s(n)\}$ sampled from signal $s(t)$, $\theta(n)$ obeys a normal distribution with variance that varies from one sample to the next. Therefore, the distribution of IP error of the observed time series $\{s(n)\}$ is SMN distributions with different variances. If the pdf of $\{\sigma_{\theta}(n)\}$ is known, the empirical distribution of IP error $\{\theta(n)\}$ for the observed time series $\{s(n)\}$ can be approximated as

$$p_m(\theta) = \sum_{k=1}^K p(\theta|\sigma_k) \pi_k, \quad (23)$$

where $\{\pi_k\}_{k=1}^K$ are the respective empirical probabilities, which are estimated from $\{A_x(n)\}$ on a finite number of values $\{\sigma_k\}_{k=1}^K$ [39]. This means that the distribution of $\{\sigma_{\theta}(n)\}$ depends on the distribution of $\{A_x(n)\}$. Note that $A_x(n)$ is the IA of the clean signal. Thus, for the observed time series $\{s(n)\}$, which is contaminated by noise, the distribution of $\{A_x(n)\}$ is difficult, if not impossible, to be obtained analytically. In this paper, we do not try to find the exact SMN of the phase error of $\{s(n)\}$ but perform simulations by considering σ_{θ} as $\sigma_{\theta} = \sigma_{w^{(b)}}/\max\{A_x(n)\}$. In other words, the SMN of the phase error is approximated by a normal distribution with a constant standard deviation $\sigma_{w^{(b)}}/\max\{A_x(n)\}$. Simulations with this assumption will be performed in Sec. V.

³In this paper, we adopt the index based on circular statistics because it will be convenient for us to deduce the effect of noise analytically. For the index based on entropy, it is difficult, if not impossible, to deduce an analytical result on the effect of noise.

With the estimated $\{\hat{\varphi}(n)\}_{n=0}^{L-1}$, the MPC is estimated as

$$\hat{\rho} = \left\{ \left[\frac{1}{L} \sum_{n=0}^{L-1} \cos \hat{\varphi}(n) \right]^2 + \left[\frac{1}{L} \sum_{n=0}^{L-1} \sin \hat{\varphi}(n) \right]^2 \right\}^{1/2}, \quad (24)$$

where L is the number of samples in $\{s(n)\}_{n=0}^{L-1}$.

Note that distribution tests of PS have been investigated from other viewpoints [37,40]. Empirical distributions of IP difference of coupled Rössler systems have been tested under the assumption that IP obeys specific distributions. But this is applicable only for special cases of PS because the assumption of the distribution of IP is not generally valid for different systems [40]. Moreover, the IPs of different samples are assumed to be independent, which is not the case for dynamical systems. The statistical properties of MPC are investigated in Ref. [37]. The distribution of the estimated MPC is approximated by a specific distribution, which is valid only for time series of a large number of samples. This distribution is dependent on two parameters, i.e., the mean angular velocity and the diffusion constant. As long as the assumptions are fulfilled and the two dependent parameters are reliably estimated, a reasonable significance level can be obtained by this model, providing a test for a nonzero synchronization index.

V. NUMERICAL RESULTS

In Sec. IV, the effect of noise in IP estimation and PS detection has been studied analytically. To validate the deduced results, we perform simulations based on two typical examples: sine waves and coupled Rössler systems.

A. Test with sine waves

We define a simple sine wave and an amplitude-modulated sine wave as

$$x_1(t) = 10 \cos(2\pi f_1 t),$$

$$x_2(t) = (10 + 4 \sin 2\pi f_a t) \cos\left(2\pi f_2 t + \frac{\pi}{2}\right), \quad (25)$$

where $f_1 = 2$ Hz, $f_2 = 2$ Hz, and $f_a = 0.2$ Hz. Two 40 000-sample time series are measured from $x_1(t)$ and $x_2(t)$, respectively, with sampling interval $\Delta t = 0.05$. The measured time series are denoted by $x_{1,2}(n\Delta t)$ and their noisy versions are denoted by $s_{1,2}(n\Delta t) = x_{1,2}(n\Delta t) + w_{1,2}(n\Delta t)$, where $w_{1,2}(n\Delta t)$ are the noise terms and assumed to be Gaussian white noise $w_{1,2} \sim N(0, \sigma_{w_{1,2}}^2)$. The noise level η is defined as $\sigma_{x_{1,2}} = \eta \sigma_{w_{1,2}}$, where $\sigma_{x_{1,2}}$ are the variances of $x_{1,2}$, and $\sigma_{w_{1,2}}$ are the variances of $w_{1,2}$, respectively. To simplify the notation, Δt is omitted and $s_{1,2}(n\Delta t)$ are written as $s_{1,2}(n)$ from now on.

The distributions of IP error $\{\theta(n)\}$ due to the added noise are illustrated in Fig. 2 and the normalities of the distributions of IP errors are tested with χ^2 goodness of fit. For $x_1(t)$, its IA is constant, and thus the distribution of IP error $\{\theta_1(n)\}$ should be a wrapped normal distribution according to Eq. (18) when the noise level is not high. For the result shown in Fig. 2(d), the p value is 0.87, and thus the null hypothesis

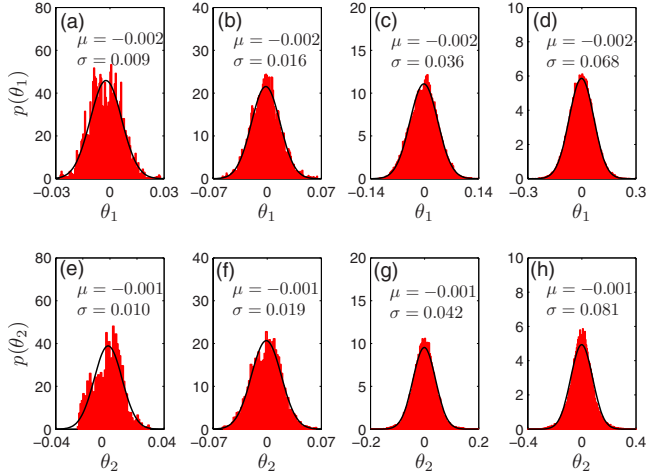


FIG. 2. (Color online) The pdfs of IP error for a sine wave (the first row) and an amplitude-modulated sine wave (the second row). The black curves are the normal distribution fits of the corresponding empirical distributions. These pdfs are calculated from the clean time series $\{x_{1,2}(n)\}$ and their corresponding noisy versions $\{s_{1,2}(n)\}$ with noise level $\eta=0.2$. The values of μ and σ marked in each panel are the means and the standard deviations of the corresponding normal fits. The filters are with nominal frequency $f_n=2$ Hz and bandwidth: (a) and (e) $\Delta f_1=0.016$ Hz, (b) and (f) $\Delta f_2=0.064$ Hz, (c) and (g) $\Delta f_3=0.256$ Hz, and (d) and (h) $\Delta f_4=1.024$ Hz. Details about the filter with Gaussian envelope can be found in Ref. [28].

(i.e., the IP error is a random time series from a normal distribution) cannot be rejected at the 5% significance level. While for the cases of Figs. 2(a)–2(c), the null hypothesis should be rejected [the p value for the case of Fig. 2(c) is 2.04×10^{-4} , and the p values for the other two cases are even much smaller]. For $x_2(t)$, its amplitude is modulated by a sine wave, and thus its IA is not constant. Then the distribution of IP error $\{\theta_2(n)\}$ is a SMN [Eqs. (22) and (23)]. The empirical distributions of the IP errors for $x_2(t)$ are illustrated in Figs. 2(e)–2(h). The p values for these four cases are very small ($<5.43 \times 10^{-16}$), which implies that the SMNs of IP errors cannot be well approximated by particular normal distributions. Note that for both $x_1(t)$ and $x_2(t)$, the narrower the bandwidth of the filter, the smaller the p value for the corresponding IP error $\{\theta(n)\}$. This may imply that the rejection of the null hypothesis for the cases of Figs. 2(a)–2(c) is due to the numerical error, which is induced by the filter with too narrow bandwidth.

B. Test with coupled Rössler systems

To illustrate the effect of noise in PS detection, the coupled Rössler systems [2]

$$\begin{aligned} \dot{x}_{1,2} &= -\varpi_{1,2}y_{1,2} - z_{1,2} + \xi(x_{2,1} - x_{1,2}), \\ \dot{y}_{1,2} &= \varpi_{1,2}x_{1,2} + \alpha y_{1,2}, \\ \dot{z}_{1,2} &= \beta + z_{1,2}(x_{1,2} - \gamma), \end{aligned} \quad (26)$$

are taken as an example, where ξ is the coupling strength. Data are integrated from variables $x_{1,2}$, using the fourth-order

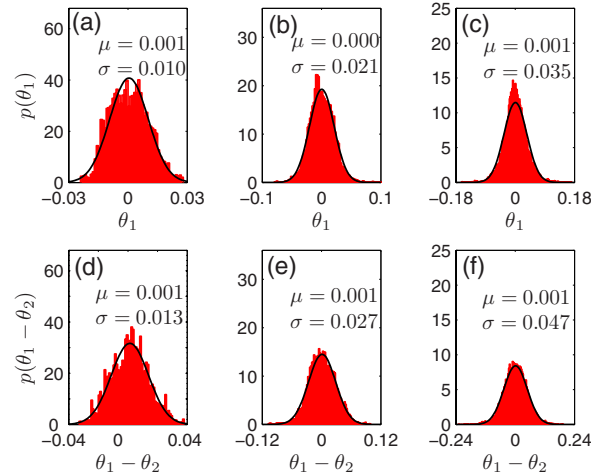


FIG. 3. (Color online) The pdfs of IP error [$p(\theta_1)$, the first row] and IP error difference [$p(\theta_1 - \theta_2)$, the second row] for the coherent Rössler time series with bandpass filter applied. The filters are with nominal frequency $f_n=0.1645$ Hz and bandwidth: (a) and (d) $\Delta f_1=0.016$ Hz, (b) and (e) $\Delta f_2=0.064$ Hz, and (c) and (f) $\Delta f_3=0.256$ Hz. These pdfs are calculated from the clean Rössler time series and their corresponding noisy time series with noise level $\eta=0.2$. With coupling strength $\xi=0.035$, the coupled systems are synchronous.

Runge-Kutta method with sampling interval $\Delta t=0.05$. The initial values are set randomly, and 40 000 samples, after discarding the first 10 000 samples, are adopted for analysis. Noise is added to the measured time series to generate noisy time series as done in Sec. V A above. Two cases of the coupled Rössler systems are studied: (1) coherent systems with parameters $\alpha=0.15$, $\beta=0.2$, $\gamma=10$, $\varpi_1=1.015$, and $\varpi_2=0.985$ and (2) noncoherent systems with parameters $\alpha=0.25$, $\beta=0.2$, $\gamma=10$, $\varpi_1=1.015$, and $\varpi_2=0.985$.

With coupling strength $\xi=0.035$, the coherent systems are synchronized [1]. The spectral peak of the measured data is located around frequency 0.1645 Hz. So the bandpass filter of nominal frequency $f_n=0.1645$ Hz is utilized. The distributions of IP error for different cases are illustrated in Fig. 3 and normality tests show that the null hypothesis should be rejected for all these cases [χ^2 goodness of fit, the p value for the case of Fig. 3(f) is 1.15×10^{-8} , and the p values for other cases are even smaller]. These results are as expected. As discussed in Sec. IV, the distribution of IP error $\{\theta(n)\}$ is actually a SMN, which is affected by the distribution of IA $A_x(n)$. However, IA $A_x(n)$ is not constant in most cases [e.g., see Fig. 4]. So the distribution of IP error $p(\theta)$ and the distribution of IP error difference $p(\theta_1 - \theta_2)$ usually cannot be well approximated by particular normal distributions.

As mentioned in Sec. IV, it is difficult to get an analytical form of the SMN of IP error with only an observed time series. So in studying the effect of noise in PS detection, we perform simulations under the assumption that the IA of the time series is a constant, and the SMN of the IP error can be approximated by a normal distribution. Figures 5–7 show the PS indices of numerical estimates [i.e., estimated from the IP estimates $\{\hat{\varphi}(n)\}$ via Eq. (24)] and their corresponding theoretical predictions [i.e., via Eq. (21)] for synchronous systems, weakly synchronous systems, and nonsynchronous

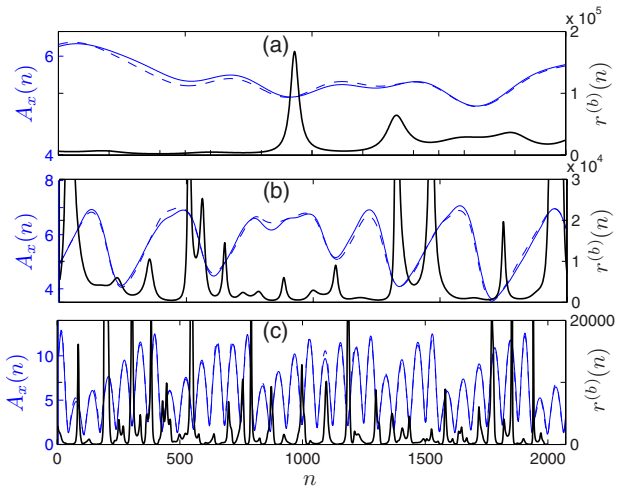


FIG. 4. (Color online) The IA $A_x(n)$ and iSNR $r^{(b)}(n)$ of the coherent Rössler time series with bandpass filter applied. The filters are with nominal frequency $f_n=0.1645$ Hz and bandwidth: (a) $\Delta f_1=0.016$ Hz, (b) $\Delta f_2=0.064$ Hz, and (c) $\Delta f_3=0.256$ Hz. In each panel, the blue (gray) solid curve is the IA (the left y axis) estimated from the clean data, the blue (gray) dashed curve is the IA estimated from the noisy version of the clean data, and the thick black curve is the corresponding iSNR (the right y axis). The coupling strength is $\xi=0.035$ and the noise level is $\eta=0.2$.

systems, respectively. For these coupled coherent Rössler systems, it is shown that the theoretical predictions are consistent with the trends of numerical simulations. However, for coupled noncoherent Rössler systems, simulations show

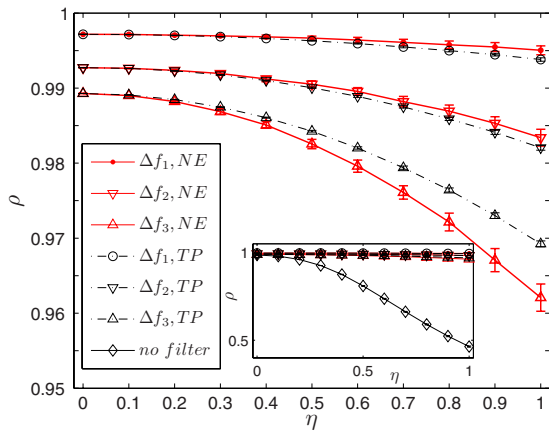


FIG. 5. (Color online) The estimated PS indices and the corresponding theoretical predictions for the coupled coherent Rössler systems with respect to the noise level η . To examine the effect of noise on PS index ρ , one pair of clean Rössler time series are generated, and for each noise level and each filter, simulations are performed based on 100 pairs of noisy Rössler time series, which are generated by adding independent and identically distributed white Gaussian noise series to that pair of clean Rössler time series. The results are plotted as mean \pm standard deviation. NE denotes the results of numerical estimates, and TP denotes the corresponding theoretical predictions. Symbol \diamond shown in the inset denotes the results obtained by the Hilbert transform with no bandpass filter applied. $\Delta f_1=0.016$ Hz, $\Delta f_2=0.064$ Hz, and $\Delta f_3=0.256$ Hz. The coupled systems are synchronous with coupling strength $\xi=0.035$.

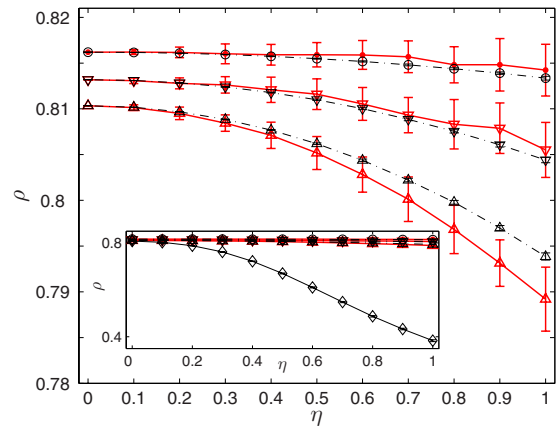


FIG. 6. (Color online) The estimated PS indices and the corresponding theoretical predictions for the coupled coherent Rössler systems with respect to the noise level η . The coupled systems are weakly synchronous with coupling strength $\xi=0.027$. Simulation strategy and the denotation of each curve as that in Fig. 5.

that the theoretical predictions are much larger than the numerical estimates, as Fig. 8 indicates. This is because the IAs of the case of noncoherent Rössler systems are far from constant, and thus the SMN of the IP error cannot be approximated by a normal distribution. Note that we have also analyzed the effect of additive noise in detecting PS of pairs of electroencephalogram signals. Results show that the theoretical predictions are not consistent with the corresponding numerical estimates, which is due to the same reason as the case of the coupled noncoherent Rössler systems, that is, the IAs are far from constant.

Moreover, Figs. 5–7 show that, with narrow bandpass filter, the estimated PS indices, as well as the theoretical predictions, are not so much degraded (compared with the results with no filter) even when the noise level is high. This implies that the bandpass filter is necessary and effective in dealing with data contaminated by additive noise. As Figs. 5 and 6 indicate, the narrower the bandpass filter, the larger the esti-

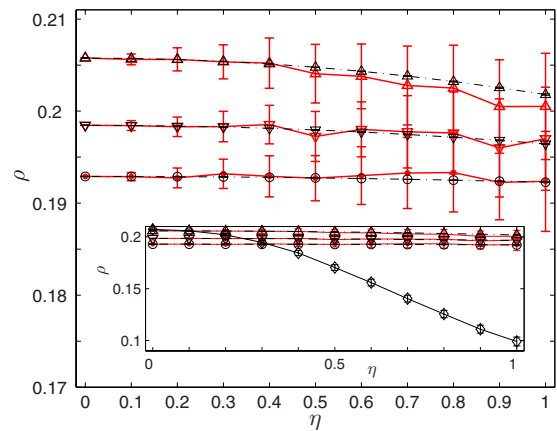


FIG. 7. (Color online) The estimated PS indices and the corresponding theoretical predictions for the coupled coherent Rössler systems with respect to the noise level η . The coupled systems are nonsynchronous with coupling strength $\xi=0.01$. Simulation strategy and the denotation of each curve are as that in Fig. 5.

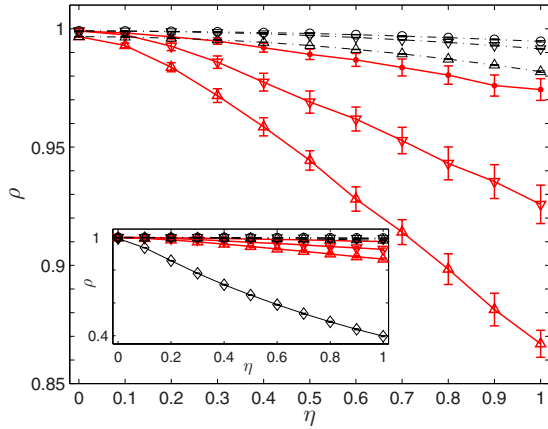


FIG. 8. (Color online) The estimated PS indices and the corresponding theoretical predictions for noncoherent Rössler systems ($\alpha=0.25$) with respect to the noise level η . The coupled systems are synchronous with coupling strength $\xi=0.2$, $f_n=0.134$ Hz. Simulation strategy and the denotation of each curve are as that in Fig. 5.

estimated PS index. This overestimation of synchronization level is introduced by the filter and has been discussed in Ref. [23]. This can be explained with the second extreme case discussed in Sec. III C. When the filter $b(t)$ becomes extremely narrow, i.e., a delta filter in the frequency domain, the components extracted by the filter from signals $s_1(t)$ and $s_2(t)$ are just the spectral components of their Fourier transform at the nominal frequency. Then the IP difference between these two components is a constant and the corresponding PS index will be unity. Generally, PS index is a relative measure to compare the synchronization level of coupled systems under different conditions (e.g., with different coupling strengths). For these coupled systems, if the same bandpass filter is applied, the estimated PS indices can indicate which coupled pairs have a higher level of synchronization than others because the overestimation induced by the same filter is likely to be the same.

However, in Fig. 7, the narrower filter gives smaller PS index. This is because for the cases of Figs. 5 and 6, the coupled Rössler systems are synchronous and weakly synchronous, respectively, and the prominent spectral components of $x_1(t)$ and $x_2(t)$ both locate in the pass band of the filter applied. In contrast, for the case of Fig. 7, the coupled Rössler systems are nonsynchronous, and due to the mismatch of parameters ($\varpi_1=1.015$, $\varpi_2=0.985$), the prominent spectral components of $x_1(t)$ and $x_2(t)$ are around 0.167 Hz and 0.1625 Hz, respectively. The filter Δf_1 , possibly as well as the filter Δf_2 , is with too narrow bandwidth, and thus greatly attenuates the prominent spectral components of $x_1(t)$ and $x_2(t)$, resulting in a lower PS index.

In Sec. III B, it has been suggested that the bandwidth of the filter should satisfy $\frac{\Delta f}{2} < f_n$ so that the filtered signal could fulfill the Bedrosian theorem. This requirement gives the upper bound of the bandwidth of the filter. In real applications, though the filter with narrower bandwidth may suppress more noise, it does not mean that the filter with narrower bandwidth always works better, as the simulation results in Figs. 2(a)–2(c) and 7 indicate. For the observable signal $s(t)$ of time duration T_d , the physical frequency reso-

lution of the spectra estimated by the Fourier transform is no less than $\frac{1}{T_d}$ [41]. Therefore, the bandwidth Δf must satisfy $\Delta f > \frac{1}{T_d}$. In addition, the prominent spectral components of the signals should locate in the pass band of the filter. So in real applications, tradeoffs must be made in determining the bandwidth of the filter.

VI. CONCLUSION

In this paper, we study the definition of IP and the effect of noise in PS detection from the viewpoints of signal processing and circular statistics. We show that several definitions of IP can be unified into one framework: applying a specific filter to the time series and defining IP as the argument of the output of the filter. Further, constraints on IP definitions are given and the relationship among several IP definitions is discussed. With the unified framework, the estimate error of IP, which is due to noise, is shown to obey SMN distributions. The estimate of MPC is shown to be degraded by a factor, which is determined by only the level of in-band noise, under the assumption that the IA of the observed signal is a constant and thus the SMN of the IP error can be approximated by a normal distribution. These results are further verified by numerical simulations and discussions on the bandwidth of the filter are given. For general cases, the SMN of the IP error cannot be approximated by a normal distribution. The empirical distribution is difficult, if not impossible, to be deduced theoretically. So for real applications, it is difficult to get a good theoretical prediction of synchronization level. Nevertheless, the deduced analytic results can give an implication (theoretically) of how and by how much the noise affects PS detection.

Moreover, the significance of the estimated PS index should be tested before it can be claimed that the estimated index implies that the underlying coupled systems are really in PS. Several methods, including surrogate tests, have been proposed to address this problem [10,37,40,42]. Most of the traditional surrogate methods only mimic the linear properties such as the individual spectra of each original signal or the cross spectra of the original signal pair [42]. The surrogate data generated by these surrogate methods usually obey a particular linear stochastic process. However, PS characterizes the mutual adaption of coupled oscillators but not the relationship among stochastic processes. Thus, these surrogate tests do not work well for PS detection. Recently, a method called twin surrogates has been proposed based on recurrence properties of the original data [43]. This method can mimic both the linear and nonlinear properties of the original oscillators and seems promising to give significance test for PS detection.

ACKNOWLEDGMENTS

The authors thank Shanbao Tong for a critical reading of the paper. This work was supported by an internal research grant provided by the Hong Kong Polytechnic University (Grant No. G-YG35), the Key Project of Chinese Ministry of Education (Grant No. 109059), and a grant from the National Natural Science Foundation of China (Grant No. 60901025).

- [1] M. G. Rosenblum, A. S. Pikovsky, and J. Kurths, *Phys. Rev. Lett.* **76**, 1804 (1996).
- [2] P. Tass, M. G. Rosenblum, J. Weule, J. Kurths, A. Pikovsky, J. Volkman, A. Schnitzler, and H.-J. Freund, *Phys. Rev. Lett.* **81**, 3291 (1998).
- [3] R. T. Canolty, E. Edwards, S. S. Dalal, M. Soltani, S. S. Nagarajan, H. E. Kirsch, M. S. Berger, N. M. Barbaro, and R. T. Knight, *Science* **313**, 1626 (2006).
- [4] M. Le Van Quyen and A. Bragin, *Trends Neurosci.* **30**, 365 (2007).
- [5] D. J. DeShazer, R. Breban, E. Ott, and R. Roy, *Phys. Rev. Lett.* **87**, 044101 (2001).
- [6] I. Z. Kiss, Q. Lv, and J. L. Hudson, *Phys. Rev. E* **71**, 035201(R) (2005).
- [7] S.-B. Shim, M. Imboden, and P. Mohanty, *Science* **316**, 95 (2007).
- [8] C. Hammond, H. Bergman, and P. Brown, *Trends Neurosci.* **30**, 357 (2007).
- [9] A. Pikovsky, M. Rosenblum, and J. Kurths, *Synchronization: A Universal Concept in Nonlinear Sciences* (Cambridge University Press, England, 2001).
- [10] J. M. Hurtado, L. L. Rubchinsky, and K. A. Sigvardt, *J. Neurophysiol.* **91**, 1883 (2004).
- [11] R. Brown and L. Kocarev, *Chaos* **10**, 344 (2000).
- [12] R. Quiñero, A. Kraskov, T. Kreuz, and P. Grassberger, *Phys. Rev. E* **65**, 041903 (2002).
- [13] T. Pereira, M. S. Baptista, and J. Kurths, *Phys. Rev. E* **75**, 026216 (2007).
- [14] J. Sun, J. Zhang, J. Zhou, X. Xu, and M. Small, *Phys. Rev. E* **77**, 046213 (2008).
- [15] T. Kreuz, F. Mormann, R. G. Andrzejak, A. Kraskov, K. Lehnertz, and P. Grassberger, *Physica D* **225**, 29 (2007).
- [16] M. Winterhalder, B. Schelter, J. Kurths, A. Schulze-Bonhage, and J. Timmer, *Phys. Lett. A* **356**, 26 (2006).
- [17] A. G. Rossberg, K. Bartholomé, and J. Timmer, *Phys. Rev. E* **69**, 016216 (2004).
- [18] J. Kurths, M. C. Romano, M. Thiel, G. V. Osipov, M. V. Ivanchenko, I. Z. Kiss, and J. L. Hudson, *Nonlinear Dyn.* **44**, 135 (2006).
- [19] A. E. Hramov and A. A. Koronovskii, *Chaos* **14**, 603 (2004).
- [20] T. Pereira, M. S. Baptista, and J. Kurths, *Phys. Lett. A* **362**, 159 (2007).
- [21] P. J. Loughlin, *J. Acoust. Soc. Am.* **105**, 264 (1999).
- [22] P. M. Oliveira and V. Barroso, *J. Franklin Inst.* **337**, 303 (2000).
- [23] L. Xu, Z. Chen, K. Hu, H. E. Stanley, and P. C. Ivanov, *Phys. Rev. E* **73**, 065201(R) (2006).
- [24] G. V. Osipov, B. Hu, C. Zhou, M. V. Ivanchenko, and J. Kurths, *Phys. Rev. Lett.* **91**, 024101 (2003).
- [25] D. Vakman, *IEEE Trans. Signal Process.* **44**, 791 (1996).
- [26] L. Cohen, *Time-Frequency Analysis* (Prentice-Hall, Englewood Cliffs, NJ, 1995).
- [27] B. Boashash, *Proc. IEEE* **80**, 520 (1992).
- [28] D. Vakman, *IEEE Trans. Instrum. Meas.* **43**, 668 (1994).
- [29] E. Bedrosian, *Proc. IEEE* **51**, 868 (1963).
- [30] A. H. Nuttall and E. Bedrosian, *Proc. IEEE* **54**, 1458 (1966).
- [31] S. Mallat, *A Wavelet Tour of Signal Processing* (Academic Press, San Diego, CA, 1998).
- [32] H. Kantz and T. Schreiber, *Nonlinear Time Series Analysis*, 2nd ed. (Cambridge University Press, England, 2003).
- [33] A. Bruns, *J. Neurosci. Methods* **137**, 321 (2004).
- [34] N. M. Blachman, *Proc. IRE* **41**, 748 (1953).
- [35] B. C. Lovell and R. C. Williamson, *IEEE Trans. Signal Process.* **40**, 1708 (1992).
- [36] S. R. Jammalamadaka and A. SenGupta, *Topics in Circular Statistics* (World Scientific, Singapore, 2001).
- [37] B. Schelter, M. Winterhalder, J. Timmer, and M. Peifer, *Phys. Lett. A* **366**, 382 (2007).
- [38] W. R. Bennett, *Proc. IRE* **44**, 609 (1956).
- [39] H. Hamdan, *Commun. Stat: Theory Meth.* **35**, 407 (2006).
- [40] C. Allefeld and J. Kurths, *Int. J. Bifurcation Chaos Appl. Sci. Eng.* **14**, 405 (2004).
- [41] S. J. Orfanidis, *Introduction to Signal Processing* (Prentice Hall, Englewood Cliffs, NJ, 1996).
- [42] M. Palus, *Phys. Lett. A* **235**, 341 (1997).
- [43] M. Thiel, M. C. Romano, J. Kurths, M. Rolf, and R. Kliegl, *Europhys. Lett.* **75**, 535 (2006).